



Predictive screening model for potential vector-mediated transport of cationic substrates at the blood–brain barrier choline transporter

Werner J. Geldenhuys^{a,b}, Vamshi K. Manda^a, Rajendar K. Mittapalli^a, Cornelis J. Van der Schyf^b, Peter A. Crooks^c, Linda P. Dwoskin^c, David D. Allen^b, Paul R. Lockman^{a,*}

^a Department of Pharmaceutical Sciences, Texas Tech University Health Sciences Center, School of Pharmacy, Amarillo, TX 79106-1712, USA

^b Department of Pharmaceutical Sciences, Northeastern Ohio Universities College of Pharmacy, Rootstown, OH 44272, USA

^c Department of Pharmaceutical Sciences, College of Pharmacy, University of Kentucky, Lexington, KY 40536-0082, USA

ARTICLE INFO

Article history:

Received 30 November 2009

Accepted 18 December 2009

Available online 28 December 2009

Keywords:

Drug screening

Drug bioavailability

Carrier-mediated transport

Smoking cessation

Nicotinic receptor antagonists

Quaternary ammonium analogs

ABSTRACT

A set of semi-rigid cyclic and acyclic bis-quaternary ammonium analogs, which were part of a drug discovery program aimed at identifying antagonists at neuronal nicotinic acetylcholine receptors, were investigated to determine structural requirements for affinity at the blood–brain barrier choline transporter (BBB CHT). This transporter may have utility as a drug delivery vector for cationic molecules to access the central nervous system. In the current study, a virtual screening model was developed to aid in rational drug design/ADME of cationic nicotinic antagonists as BBB CHT ligands. Four 3D-QSAR comparative molecular field analysis (CoMFA) models were built which could predict the BBB CHT affinity for a test set with an $r^2 < 0.5$ and cross-validated q^2 of 0.60, suggesting good predictive capability for these models. These models will allow the rapid in silico screening of binding affinity at the BBB CHT of both known nicotinic receptor antagonists and virtual compound libraries with the goal of informing the design of brain bioavailable quaternary ammonium analogs that are high affinity selective nicotinic receptor antagonists.

© 2009 Elsevier Ltd. All rights reserved.

Introduction: Structural modification of the nicotine molecule via N-n-alkylation converts it from an agonist to an antagonist at neuronal nicotinic acetylcholine receptors (nAChRs).¹ Despite the discovery of numerous novel nAChR antagonists² that may have potential as therapeutic agents in smoking cessation^{3,4} the presence of one or more quaternary ammonium moieties in such molecules suggest that these compounds will have poor brain bioavailability.

For centrally acting drugs, the blood–brain barrier (BBB) is the limiting factor in central nervous system (CNS) accumulation, with >98% of small molecules being excluded because they have poor diffusion through the BBB or are subject to efflux through a variety of carrier-mediated mechanisms.⁵ This restriction in CNS access is even more notable for hydrophilic or charged compounds, where the blood-to-brain extraction related to diffusion is commonly less than 1%.^{6–8} This exclusionary property of the BBB is predicted to strongly inhibit the passive brain penetration of the quaternary ammonium nAChR antagonists into the CNS given that such compounds bear a permanent cationic charge. While carefully planned lipophilic chemical modifications could increase the octanol–water partition coefficient of such drugs and theoretically increase brain accumulation, in reality there will only be a limited increase in the

in vivo brain volume of distribution. This is secondary to an overall increase in the partitioning of the drug to other tissues, and a resultant decreased total exposure of the drug to brain.⁹

An alternative drug design strategy would be to modify the charged molecule to enable it to utilize a native BBB nutrient transporter as a CNS ‘Trojan horse’ drug delivery vector.⁸ Recent work has suggested that the BBB choline transporter (CHT) may be a suitable vector for the CNS delivery of cationic drugs, because choline plasma concentrations are only approximately 25% of the K_m of that for choline at the BBB CHT; thus, the system is free to transport other molecules without interrupting the vital supply of choline to the CNS.^{10,11} The BBB CHT is thought to be responsible for the intracellular transport of the quaternary ammonium ellipticines that are cytotoxic to isolated human brain tumor cells¹² and the blood-to-brain translocation of the N-n-alkylnicotinium analog, N-n-octylnicotinium iodide (NONI).¹⁰ Of major significance to this report is that recent drug discovery studies have identified a novel, potent bis-quaternary ammonium nAChR antagonist, N,N'-dodecane-1,12-diyl-bis-3-picolinium dibromide (bPiDDb; Fig. 1), which is currently being investigated as a lead compound for smoking cessation.¹³ bPiDDb has been shown to inhibit nAChR-mediated nicotine-evoked [³H]-dopamine release with an IC_{50} of 2–5 nM,^{14–19} and has good brain bioavailability secondary to BBB influx via the CHT.^{15,20}

For drug discovery purposes, access to the 3D structure of the BBB CHT would provide an ideal de novo design platform for

* Corresponding author. Tel.: +1 806 356 4750x227; fax: +1 806 356 4770.

E-mail address: paul.lockman@ttuhsc.edu (P.R. Lockman).

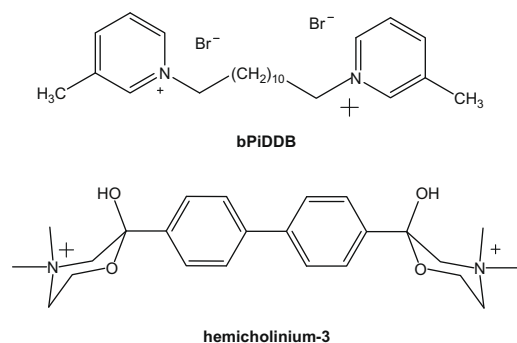


Figure 1. Structure of the bis-quaternary ammonium compounds, *N,N'*-dodecyl-bis-picolinium bromide (bPiDDB) and hemicholinium-3, high affinity bis-quaternary ammonium inhibitors of BBB CHT.

identifying molecules that could be potential substrates for this transporter. Unfortunately, unlike the neuronal high affinity CHT,^{21,22} the BBB CHT has not been cloned. In addition, the neuronal high affinity CHT has significantly different kinetic parameters compared to the BBB CHT,¹¹ suggesting that these are two different proteins. Thus, only indirect methods can be used to determine structural requirements for substrates at the BBB CHT.²³ In earlier studies the 3D quantitative structure–activity relationship approach of Cramer²⁴ (i.e., comparative molecular field analysis; CoMFA) was used to develop a model that provided insight into the structural requirements of molecules with affinity for the BBB CHT,²⁵ including a series of bis-quaternary ammonium compounds that may bind to two distinct adjacent sites on the transporter (Fig. 2).²⁶ However, the analogs used in these studies were flexible molecules affording multiple molecular conformations resulting in correlative values that were not able to predict transporter interaction. This current study expands the earlier BBB CHT CoMFA models²⁶ to include novel semi-rigid cyclic and acyclic bis- and *mono*-quaternary ammonium compounds (Tables 1–3) that are conformationally restrained analogs of bPiDDB, and which reduce the number of conformations that the substrate can present to the transporter. In addition, these novel substrates all have a cation quaternary ammonium moiety, which is assumed to be involved in the major interaction with the BBB CHT.

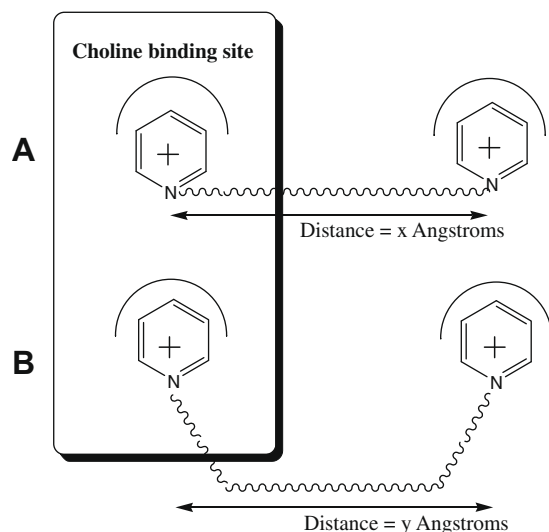
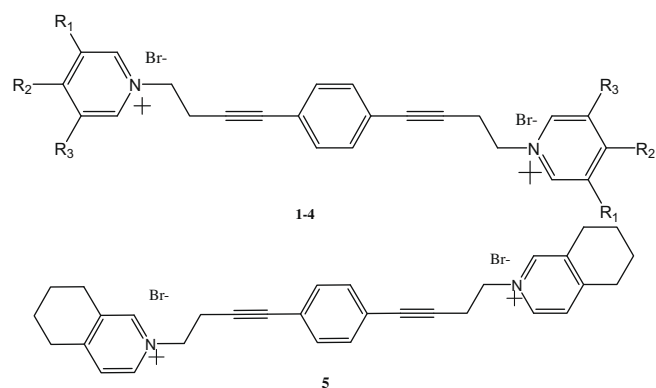


Figure 2. Schematic representation of the possible binding conformations which the compounds in this study could adopt, when binding to the blood–brain barrier choline transporter. The bis-cationic nitrogen interaction sites are either (1) the intramolecular *N–N* distance of the acyclic compounds when fully extended, or (2) the intramolecular *N–N* distance in the cyclic compounds.

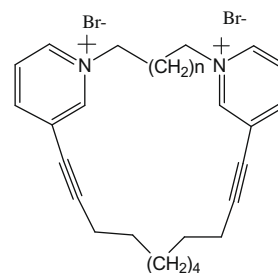
Table 1



Compound	R ₁	R ₂	R ₃	log <i>K_i</i> (μM)
1	CH ₃	—	—	0.595
2	—	CH ₃	—	0.929
3	CH ₃	CH ₃	—	0.924
4	CH ₃	—	CH ₃	0.867
5	—	—	—	0.732

Structures of conformationally restrained bis-quaternary ammonium analogs **1–5**. The mean apparent Log *K_i* at the BBB CHT are reported for in situ perfusions of each compound at concentrations of 250 μM (*n* = 4–5).

Table 2



Compound	<i>N</i>	Log <i>K_i</i> (μM)
6	8	−0.0969
7	4	1.529
8	7	0.146
9	9	1.182

Structures of conformationally restrained cyclic bis-quaternary ammonium analogs **6–9**. The mean apparent Log *K_i* at the BBB CHT are reported for in situ perfusions of each compound at concentrations of 250 μM (*n* = 4–5).

The long-term goal of our studies is to develop an in silico virtual screening model to identify quaternary ammonium substrates that will penetrate the CNS utilizing the BBB CHT. The availability of this model will allow virtual compounds to be identified that have desirable BBB CHT binding properties prior to synthesis and eliminating the need for conventional time and resource consuming structure–activity studies. This model will provide a more streamlined process for identifying compounds with optimal BBB CHT binding properties that are worthy of chemical synthesis and pharmacological evaluation. In addition, this general modeling approach may also be applicable to other nutrient or native transporters at the BBB in similar drug discovery programs.

Results: Results of the CoMFA studies are shown in Table 4. The contour CoMFA maps of Model 1 are shown in Figure 4A. This model includes the choline compounds used in an original dataset,²⁵ as well as the quaternary ammonium compounds (Table 3). Model 1 showed a non-cross validated *r*² of 0.854 (S.E.E = 0.449) and a cross-validated *q*² value of 0.392 (S.E.P._{CV} = 0.916), demonstrating

Table 3

Compound Log K_i (μ M)		Compound Log K_i (μ M)	
10 2.58		19 2.56	
11 2.69		20 2.54	
12 1.92		21 1.93	
13 1.81		22 1.34	
14 2.0		23 1.20	
15 1.37		24 2.09	
16 1.75		25 1.63	
17 1.98		26 1.26	
18 1.86		27 1.73	

Structures of miscellaneous bis-quaternary ammonium analogs **10–27**. The mean apparent Log K_i at the BBB CHT are reported for in situ perfusions of each compound at concentrations of 250 μ M ($n = 4–5$). All the compounds shown in the table were prepared as bromine salts (anion not shown).

a significant correlation between actual and predicted BBB CHT affinity values. The steric and electrostatic contributions are illustrated in Figure 4A and show a large green polyhedron surrounding the space where bPiDDB was used as an alignment motif. A green area surrounds the 3-methyl substituents of the pyridinium rings of bPiDDB, suggesting that this area might be amenable to structural modification by substitution of bulkier substituents (e.g.,

ethyl, propyl). Additionally, a yellow area surrounds the region where an azaaromatic 4-substituent would be located, suggesting that bulky substituents attached at this position would likely decrease affinity. A large blue polyhedron surrounds the two cationic pyridinium groups, emphasizing the importance of the contribution of the cationic nitrogens in these compounds to overall transporter affinity.

Table 4

Parameter	CoMFA			
	Model 1	Model 2	Model 3	Model 4
q^2_{cv}	0.392	0.455	0.435	0.447
S.E.P. _{cv}	0.916	0.652	0.891	0.867
Components	5	5	5	4
Non-cross validated r^2	0.854	0.966	0.857	0.781
S.E.E.	0.449	0.164	0.448	0.546
F-test	57.297	112.469	62.547	47.127
<i>Contribution fields</i>				
Steric	0.690	0.639	0.704	0.715
Electrostatic	0.310	0.361	0.296	0.285

Results of the CoMFA partial least squares analysis for BBB CHT binding affinity (Non-cross validated r^2 values, with the S.E.E. reported for variance) and for predictive binding q^2 at the BBB CHT with variances reported as the standard error of prediction S.E.P._{cv} for bis-quaternary ammonium analogs. The contribution of the steric and electrostatic fields generated through CoMFA are shown with the relative contributions represented in a 3D coefficient map.

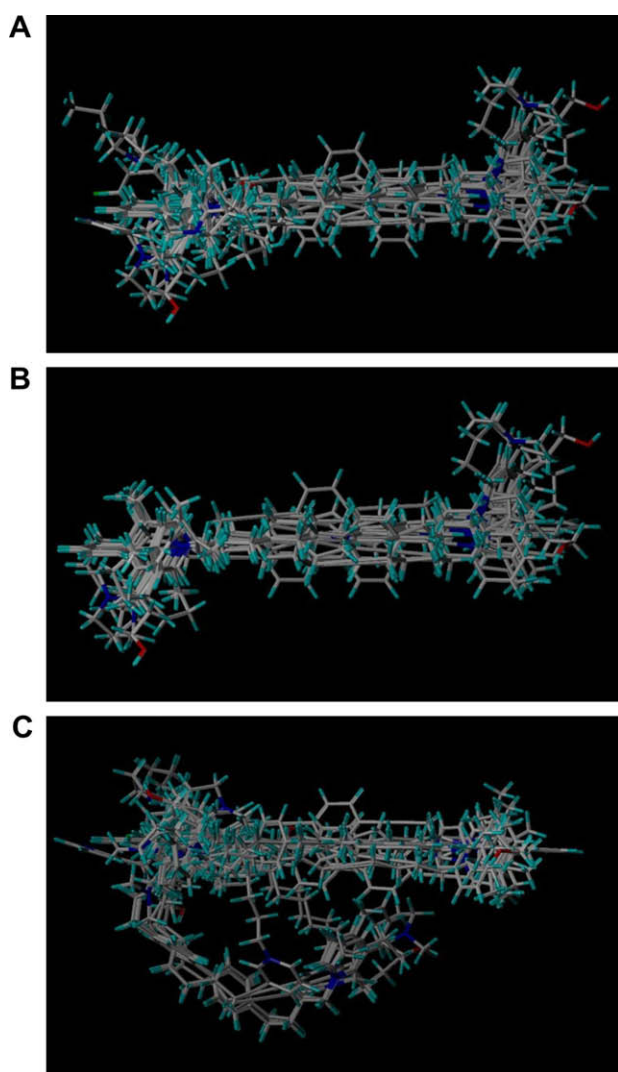


Figure 3. Alignment of compounds. Briefly, compounds were aligned with respect to bPiDDB (Fig. 1), by manually fitting the cationic nitrogens and the aromatic pyridinium rings, such that the substituents on all azaaromatic rings were aligned.⁴⁵ Three alignment perspectives are shown: (1) choline derivative, acyclic bis-quaternary ammonium compounds aligned (Model 1), (2) acyclic quaternary ammonium compounds aligned without the choline derivatives (Model 2) and (3) all quaternary ammonium compounds aligned (Models 3 and 4).

The contour CoMFA maps of Model 2 are shown in Figure 4B. This model includes only bis-quaternary ammonium compounds (Table 3), with no cyclic compounds included (e.g., those shown in Table 2). Model 2 had a non-cross validated r^2 of 0.966 (S.E.E. = 0.164) and a cross-validated q^2 value of 0.455 (S.E.P._{cv} = 0.652, Table 4), demonstrating a significant correlation between actual and predicted BBB CHT affinity values. Steric contributions are apparent, as indicated by the large green polyhedron surrounding the bPiDDB molecule, which was used as the starting structure for the alignments of the bis-quaternary series of compounds (Table 3). Favorable steric interactions (green) can be seen surrounding the 3-methyl substituents of bPiDDB, and alongside the C₁₂ *n*-alkyl linker unit connecting the two cationic N atoms. Unfavorable steric regions are observed around the 4-position of the pyridinium ring.

In Model 3 (Fig. 4C), the choline compounds from the original data set²⁵ were included, in addition to acyclic bis-quaternary ammonium compounds (Tables 1 and 3), to develop the CoMFA maps. Model 3 shows a significant correlation between actual and predicted BBB CHT affinity values with a cross-validated q^2 value of 0.435 and a non-cross validated r^2 of 0.857 (S.E.E. = 0.448, Table 4). A large sterically favorable area is observed around the 3-position of bPiDDB, which overlaps with the C₁₂ *n*-alkyl linker area. Two large blue areas are observed around the cationic pyridinium moieties, suggesting that positively charged N atoms represent the most important interaction with BBB CHT.

Figure 4D shows the contour CoMFA maps of Model 4. This model includes choline compounds that were used in our original data set,²⁵ together with new cyclic (Table 2) and acyclic bis-quaternary ammonium compounds (Table 1 and 3). However, in contrast with Model 3, six of the bis-quaternary ammonium compounds were aligned with the cyclic compounds in a bucket conformation. Model 4 shows a cross-validated q^2 value of 0.447 and a non-cross validated r^2 of 0.781 (S.E.E. = 0.546) (Table 4), demonstrating a significant correlation between actual and predicted BBB CHT affinity values.

Discussion: Data presented in the current study demonstrate that despite the structural diversity of the compounds illustrated in Tables 1–3, all compounds which contain at least one cationic center bind with varying degrees to the BBB CHT. In addition, and of major significance, is that binding affinity (log K_i) of such quaternary ammonium compounds can now be predicted using an *in silico* approach (Fig. 5). Thus, this methodology has the capability of predicting the affinity of similar molecules at the BBB CHT, and in this respect, may be a useful *in silico* screen for predicting brain bioavailability of virtual libraries of novel cationic CNS agents.

The primary substrate requirements for binding to the BBB CHT that have been previously described in the literature are (1) the presence of a cationic nitrogen in the molecule;²⁵ (2) a hydrophobic interaction; and (3) the presence of at least one hydroxyl group located approximately 3.26–3.30 Å away from the cationic nitrogen.^{7,35,36} To indirectly evaluate the interaction between the BBB CHT and the synthesized compounds, three models were constructed based on the following assumptions (Fig. 2): (1) the quaternary ammonium compounds bind to the same site as choline at the BBB CHT; (2) the second cationic interaction site in the bis-quaternary ammonium compounds is located distally from the first, at a distance equal to the entire length of the individual acyclic compounds, or equal to the distance between the cationic nitrogens in cyclic compounds; and (3) at least one of the cationic nitrogens represents a common structural feature that interacts with an anionic region in the binding site.

The data herein confirms the previous findings³⁷ that the interaction between the quaternary ammonium nitrogen in the above compounds and an anionic region on the BBB CHT binding site is

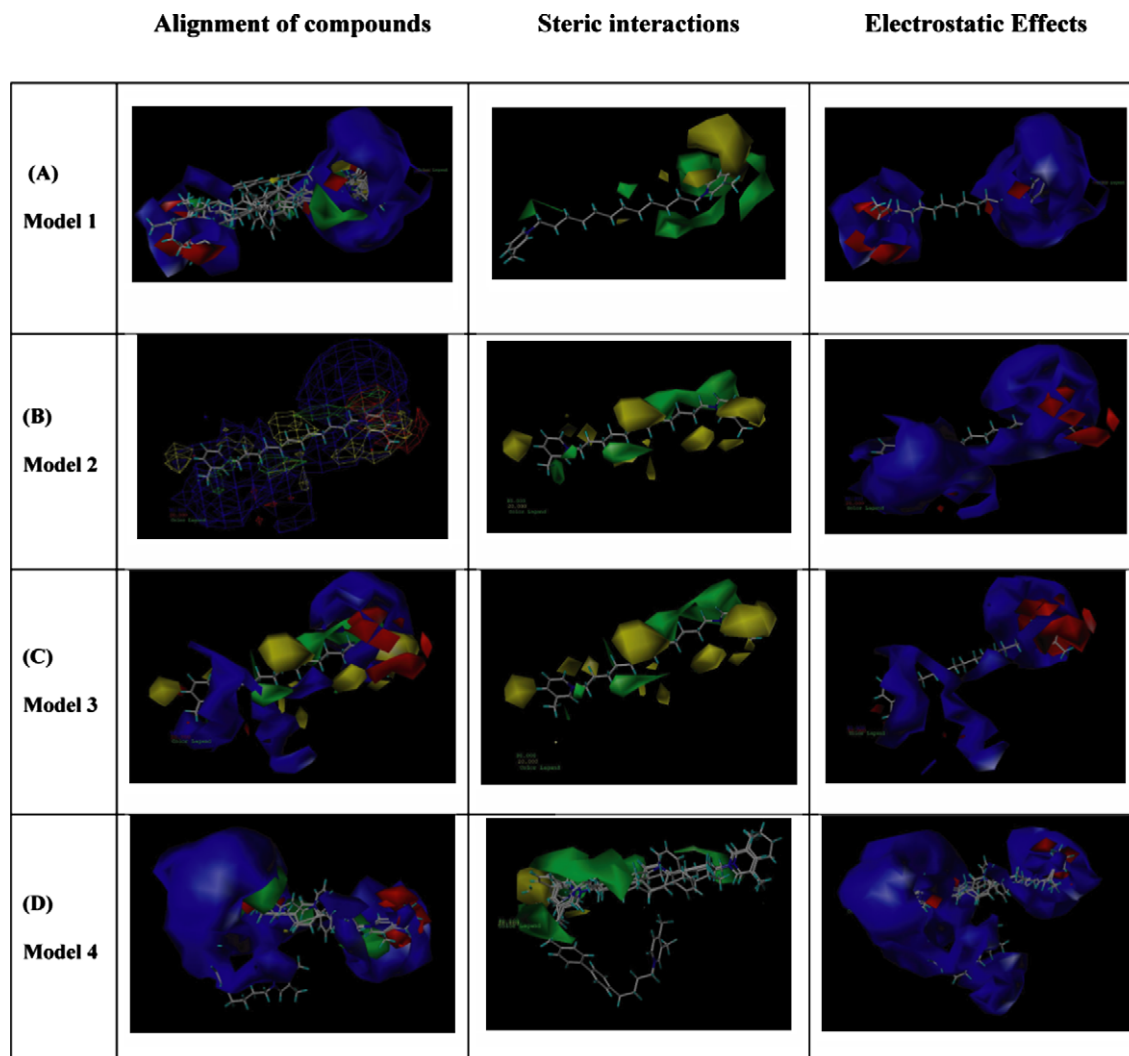


Figure 4. (a–d) Contour renditions of CoMFA maps for Models 1–4. Steric fields shown: green areas indicate regions where bulky substituents can be accommodated in a sterically favorable way, and yellow in an unfavorable way. Electrostatic fields are shown: blue areas favorably accommodate cationic groups, and red areas are unfavorable. Column 1 shows the steric and electrostatic interactions (test compounds shown docked), column 2 shows steric interactions with bPiDB shown docked, and column 3 shows the electrostatic fields at the CHT with bPiDB docked.

the primary predictor for transporter interaction. However, the focus of the current study is on modeling the interaction of bis-quaternary ammonium compounds with the BBB CHT. In this respect, it has been suggested that there is a second anionic binding region within close proximity to the primary anionic binding region.⁷ This hypothesis is based upon data showing that when two quaternary nitrogen atoms are separated by a flexible methylene linker unit, there can be an ~50 to 100-fold greater affinity for the transporter compared to choline.^{38–40} For example, hemicholinium-3 (Fig. 1), a bis-quaternary ammonium compound, interacts with the high affinity choline transporter 100–300-fold more potently compared to the structurally related monomeric compound, hemicholinium-15.^{37,41} This current study affords data that are consistent with the above hypothesis, in that no loss of binding affinity for the bis-quaternary ammonium analogs was observed when compared to the affinity of the monomeric quaternary ammonium compounds. Several bis-quaternary ammonium compounds had significantly higher affinity than choline for the BBB CHT. The novel semi-rigid and cyclic bis-analogs shown in Tables 1 and 2 generally also had higher affinity for the choline transporter than the *mono*-quaternary ammonium compounds shown in Table 3. Since two cationic groups appear to have an ‘additive’ effect on affinity for the BBB

CHT, two sites of interaction for these compounds are suggested (Fig. 2). Furthermore, since [³H]-choline was used as a ligand for determining binding, it appears that the same binding pocket is shared by the bis-quaternary ammonium compounds and choline, that is, the second binding site is not specific for bis-quaternary ammonium compounds.

Generally, the more conformationally rigid compounds appear to have greater affinity than the more conformationally flexible compounds. This observed improvement in binding affinity with the bis-quaternary ammonium compounds suggests that the BBB CHT incorporates a second anionic binding pocket, or alternatively, that the BBB CHT functions as a dimeric protein complex with closely associated anionic binding sites. The anionic binding sites associated with the dimeric protein complex are also available to interact with *mono*-quaternary ammonium analogs. This type of interaction has been observed with the monoamine oxidase enzyme (MAO-B), where only after X-ray crystallography was it determined that this enzyme exists as a dimeric complex when it interacts with substrate molecules.⁴²

The second structural characteristic that results in an increased affinity at the BBB CHT appears to be a hydrophobic interaction around the anionic binding site that accommodates the quaternary

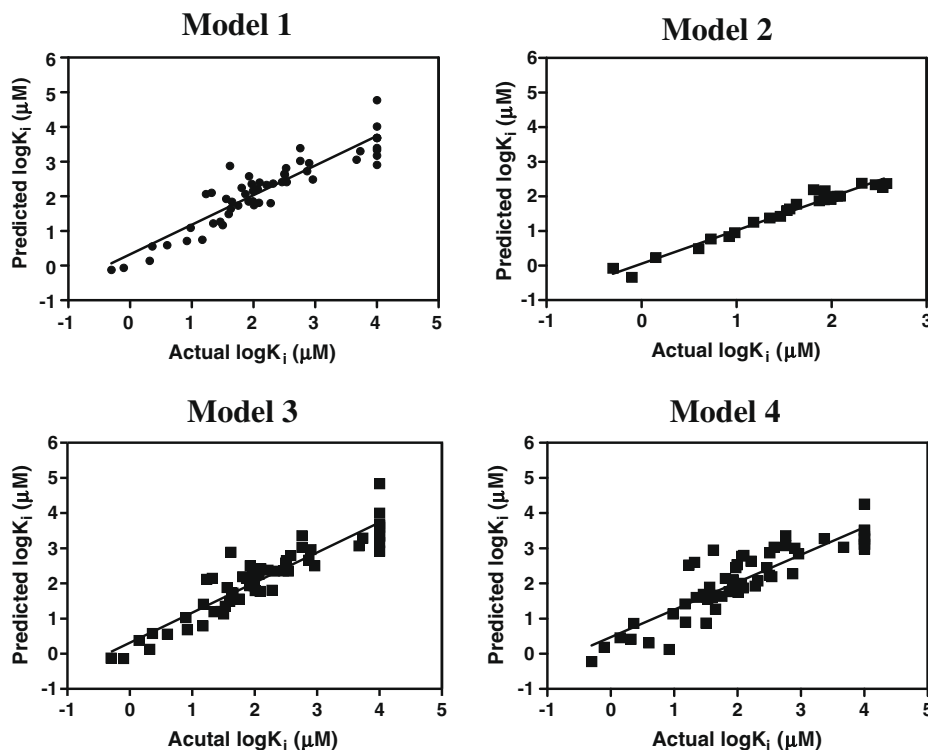


Figure 5. Correlation between the actual and predicted $\log K_i$ values for the training sets used to validate the individual CoMFA models. Linear correlation for the test sets were Model 1 ($r^2 = 0.854$, $p < 0.05$), Model 2 ($r^2 = 0.966$, $p < 0.05$), Model 3 ($r^2 = 0.857$, $p < 0.05$), and Model 4 ($r^2 = 0.781$, $p < 0.05$). Test compounds included: compounds **1**, **5**, **10**, **16**, and **26**.

ammonium center. A study by Dowdall⁴³ first suggested that the 2-[4-(1-pyrenyl)butyryloxy-ethyl]-trimethylammonium ion had a 20-fold greater affinity for the transporter than choline, and this was attributed to a hydrophobic binding region adjacent to the cationic interaction site.³⁶ In this respect, the current bis-quaternary ammonium compounds have a large hydrophobic group adjacent to the cationic nitrogen and demonstrate good affinity for the BBB CHT.

Lastly, several studies report the presence of a hydroxyl group approximately 3.26–3.30 Å away from the cationic nitrogen as being a second interaction site required for high affinity at the BBB CHT.^{7,35,36} However, the results reported herein, and in other studies,²⁶ demonstrate that our bis-quaternary ammonium compounds, which are devoid of hydroxyl groups, retain good affinity for the BBB CHT. These results suggest that the second but undefined interaction site may be an anionic region on the transporter that can act as both a hydrogen binding site and a site that could interact in an ionic manner with a quaternary ammonium nitrogen atom.

In summary, transporters such as the BBB CHT are polytopic membrane proteins, and therefore, difficult to crystallize.²³ Since no X-ray crystal structure of the BBB CHT is available,^{23,44} a 3D-QSAR methodology has been used to develop a virtual screening model for this transporter. This modeling approach has been used by others to investigate the serotonin transporter.²³ In order to further develop and extend previous *in silico* models of the BBB CHT, conformationally restrained compounds were also included in the current SAR study. To this end, models were generated utilizing both flexible and conformationally restrained molecules, based on the following assumptions (Fig. 2): (1) the quaternary ammonium compounds we show here bind to the same site as choline at the BBB CHT; (2) the second cationic interaction site is located distally from the first, at a distance equal to the entire length of the individual acyclic compounds, or equal to the distance between

the cationic nitrogens in the cyclic bis-quaternary ammonium compounds; and (3) at least one of the cationic nitrogens represents a common structural feature that interacts with an anionic region found in the BBB CHT binding region. One of the models (Model 3) described herein predicts that the flexible molecules used in our study interact with the BBB CHT in a fully extended conformation (i.e., lowest energy conformation with the two quaternary ammonium moieties fully extended). However, there is an inherent problems in using flexible molecules in a QSAR study since a large conformational space has to be accounted for in such studies. Utilizing more rigid compounds is one way of minimizing these problems associated with such QSAR analysis. In contrast to Model 3, Model 4 narrows down the conformational space and results in higher q^2 values compared to models generated using only conformationally flexible compounds. The use of the novel conformationally restrained molecules in this study suggests that there are two anionic binding sites are juxtaposed on the transporter protein. Finally, the *mono*- and *bis*-quaternary ammonium compounds which bind to the BBB CHT were initially developed as nAChR antagonists and potential smoking cessation agents.¹⁰ Based on the current findings, virtual libraries of nAChR antagonist molecules of similar structure can now be screened *in silico* to predict binding affinity at the BBB CHT with the goal of identifying molecules that are likely to be brain accessible for subsequent synthesis and pharmacological screening.

Experimental: The biological data presented herein were obtained utilizing the *in situ* rat brain perfusion technique described previously.^{11,27} Briefly, the uptake of [³H]-choline was determined by using short perfusions of a physiological fluid into the common carotid artery. Inhibition of brain [³H]-choline uptake was determined and expressed as K_i (μM) values. The compounds used for the inhibition studies were synthesized as described previously.^{1,2,4,16} The structures of the compounds were chosen to probe the nature and topological description of the possible binding sites

on the BBB CHT that could accommodate the cationic head groups in the test molecules. These molecules included conformationally flexible, semi-rigid and cyclic quaternary ammonium analogs (Tables 1–3).

Animals: Male Fischer-344 rats (220–330 g) were obtained from Charles River Laboratories, Inc. (Wilmington, MA). All studies were performed in accordance with the NIH guide for the Care and Use of Laboratory Animals, and were approved by the Animal Care and Use Committee of Texas Tech University Health Sciences Center.

In situ brain perfusion technique: Uptake of [^3H]-choline into brain was assessed using the in situ rat brain perfusion technique²⁷ with previously described modifications.^{11,28} Briefly, in this study, short perfusions of 60 s were used to determine brain uptake of [^3H]-choline. Once uptake values were calculated, subsequent experiments evaluated the inhibition of [^3H]-choline brain uptake by 250 μM of the appropriate quaternary ammonium analog in the perfusion fluid.

Radiochemicals: [^{14}C]-Sucrose (4.75 mCi/mmol) and [^3H]-choline (79.2 Ci/mmol, >98% purity) were obtained from PerkinElmer USA. In each experiment, [^3H]-choline was dried prior to being dissolved in perfusion buffer to remove volatile tritium contaminants, including [^3H]- H_2O .

Perfusion procedure: Rats were anesthetized with sodium pentobarbital (50 mg/kg, i.p.). A PE-60 catheter filled with heparinized saline (100 U/mL) was placed into the left common carotid artery after ligation of the left external carotid, occipital and common carotid arteries. Common carotid artery ligation was accomplished caudally to the catheter implantation site. The pterygopalatine artery remained open during the experiments.¹¹ Rat rectal temperature was monitored and maintained at 37 °C by a heating pad connected to a feedback device (YSI Indicating Controller, Yellow Springs, Ohio). The catheter to the left common carotid artery was connected to a syringe containing buffered physiologic perfusion fluid (containing [in mM]: NaCl 128, NaPO_3 2.4, NaHCO_3 29.0, KCl 4.2, CaCl_2 1.5, MgCl_2 0.9, and D-glucose 9) with 1 $\mu\text{Ci/mL}$ [^3H]-choline and 0.3 $\mu\text{Ci/mL}$ [^{14}C]-sucrose (to determine vascular volume). Perfusion fluid was filtered and warmed to 37 °C and gassed with 95% O_2 and 5% CO_2 . Immediately prior to perfusion, the pH and osmolarity of this solution were 7.35 and 290 mOsm, respectively. The perfusion fluid was infused into the left carotid artery with an infusion pump for a period of 60 s at 10 ml/min (Harvard Apparatus, South Natick, MA, USA). This perfusion rate was selected to maintain a carotid artery pressure of ~ 120 mm Hg.²⁸ After the 60 s perfusion with [^3H]-choline and its unlabeled analog, the perfusion fluid was changed immediately to tracer-free perfusion fluid for 15 s to wash out residual [^3H]-choline which had not been taken up into brain.

Rats were decapitated and cerebral samples obtained as previously described.¹¹ Briefly, the brain was removed from the skull, and the perfused cerebral hemisphere dissected on ice after removal of the arachnoid membrane and meningeal vessels. Brain regions were placed in scintillation vials and weighed. In addition, two 50 μL aliquots of perfusion fluid were transferred to a scintillation vial and the charged vial weighed. Brain and perfusion fluid samples were then digested overnight at 50 °C in 1 mL of 1 M piperidine solution. Ten ml of scintillation cocktail (Beckman, Fullerton, CA, USA) was added to each vial and the tracer contents assessed by dual-label liquid scintillation counting. Dual labeled scintillation counting of brain and perfusate samples was accomplished with correction for quench, background and efficiency.

Brain uptake of [^3H]-choline was determined by calculation of a single time point blood-to-brain transfer coefficient (K_{in}) as described^{27,29} from the following relationship:

$$K_{\text{in}} = [C_{\text{tot}} - V_{\text{v}}C_{\text{pf}}]/(C_{\text{pf}}/T) \quad (1)$$

where $C_{\text{tot}} = C_{\text{br}} + C_{\text{vas}}$, the sum of the amount of choline remaining in the perfusate in the blood–brain vessels, and the amount of choline that had penetrated into brain, respectively. Cerebral vascular volume and cerebral perfusion flow rate were determined in separate experiments, as previously described,^{30–32} where C_{pf} is perfusion fluid concentration of tracer choline, and T is the net perfusion time, with the assumption that uptake is linear. An apparent cerebrovascular permeability surface-area product (PA) was then determined using the following relationship:

$$PA = F \ln(1 - k_{\text{in}}/F) \quad (2)$$

where F is cerebral blood flow determined for each region of brain from the uptake of [^{14}C]-diazepam.³³

Inhibition of [^3H]-choline brain uptake was determined by the inclusion of unlabeled choline or quaternary ammonium analog in the perfusion fluid. Structures of the compounds evaluated are shown in Tables 1 and 3. To determine K_{i} , compounds were evaluated at initial concentrations of 250 μM , unless specifically stated otherwise, using the previously described method,³⁴ and detailed below. An apparent inhibition constant (K_{i}) for choline and the quaternary ammonium analogs was determined from the equation:

$$[(PA_0 - K_{\text{D}})/(PA_{\text{i}} - K_{\text{D}})] = 1 + C_{\text{i}}/K_{\text{i}} \quad (3)$$

assuming competitive kinetics, where PA_0 is the [^3H]-choline PA in the absence of competitor, PA_{i} is the [^3H]-choline PA in the presence of inhibitor, and C_{i} is the perfusate concentration of inhibitor. Apparent K_{i} is defined as the inhibitor concentration that reduces saturable brain [^3H]-choline influx by 50% at the tracer choline concentration ($C_{\text{pf}} \ll K_{\text{m}}$) and in the absence of other competing compounds. Earlier studies have demonstrated competition at the BBB CHT over a 0.25–12.5 μM concentration range of hemicholinium-3 (Fig. 1), the defining substrate for this transporter.¹¹

Molecular modeling: Molecular modeling studies were accomplished using the CoMFA module of SYBYL 6.91 (Tripos), utilizing a Silicon Graphics Octane unit. Molecules were energy-minimized in SYBYL using the MOPAC addition with AM1, with Gasteiger–Hückel charges added. Compounds were aligned with respect to bPiDDb (Fig. 1), by manually fitting the cationic nitrogens and the aromatic pyridinium rings, such that the substituents on all aromatic rings were aligned (Fig. 3). In earlier models, bPiDDb was aligned de novo with the native substrate choline by superimposing the cationic nitrogen atoms^{25,26}

Default values provided in the Tripos CoMFA module were used, with a 2.0 Å grid spacing, using a sp^3 carbon atom with a +1 point charge as a probe to explore the steric and electrostatic interactions at the lattice points in the grid. The default cut-off value was set at 30 kcal/mol. Statistical analysis was performed using the partial least squares method implemented in the SYBYL program. Non-cross validated (r^2) values were determined for the models using linear regression analysis (with variances reported as the standard error of estimation; S.E.E.) which are considered significant when r^2 is greater than 0.7. The cross-validated (q^2) values were obtained using a leave-one-out methodology (unless otherwise stated), and linear regression with variance reported as the standard error of prediction (S.E.P._{cv}). The q^2 values obtained were considered significant at 0.3. The 3D graphical representation of the steric and electrostatic fields generated through CoMFA are shown in Figure 4, with the relative contributions represented as a 3D coefficient map, with favored 80% steric (green) and electrostatic (blue) effects, and 20% disfavored steric (yellow) and electrostatic effects (red). Green colored areas of the map indicate where sterically bulky groups may enhance interaction affinity. Blue colored areas (80%) indicate regions where a more positively charged group will likely lead to increased binding affinity, while a red area indicates where a more negatively charged group will likely lead to

increased binding (20%). Biological data were entered as log K_i values in the spreadsheets accessed by the CoMFA routine in SYBYL.

Acknowledgements

The authors wish to thank the NIH (U19DA17548 to LPD, PAC, DDA and PRL) for their support.

References and notes

- Ayers, J. T.; Dwoskin, L. P.; Deaciuc, A. G.; Grinevich, V. P.; Zhu, J.; Crooks, P. A. *Bioorg. Med. Chem. Lett.* **2002**, 12, 3067.
- Crooks, P. A.; Ayers, J. T.; Xu, R.; Sumithran, S. P.; Grinevich, V. P.; Wilkins, L. H.; Deaciuc, A. G.; Allen, D. D.; Dwoskin, L. P. *Bioorg. Med. Chem. Lett.* **2004**, 14, 1869.
- Dwoskin, L. P.; Crooks, P. A. *J. Pharmacol. Exp. Ther.* **2001**, 298, 395.
- Dwoskin, L. P.; Sumithran, S. P.; Zhu, J.; Deaciuc, A. G.; Ayers, J. T.; Crooks, P. A. *Bioorg. Med. Chem. Lett.* **2004**, 14, 1863.
- Pardridge, W. M. *Drug Discov. Today* **2007**, 12, 54.
- Clark, D. E. *Drug Discovery Today* **2003**, 8, 927.
- Lockman, P. R.; Allen, D. D. *Drug Dev. Ind. Pharm.* **2002**, 28, 749.
- Pardridge, W. M. *Nat. Rev.* **2002**, 1, 131.
- Greig, N. H.; Genka, S.; Daly, E. M.; Sweeney, D. J.; Rapoport, S. I. *Cancer Chemother. Pharmacol.* **1990**, 25, 311.
- Allen, D. D.; Lockman, P. R.; Roder, K. E.; Dwoskin, L. P.; Crooks, P. A. *J. Pharmacol. Exp. Ther.* **2003**, 304, 1268.
- Allen, D. D.; Smith, Q. R. *J. Neurochem.* **2001**, 76, 1032.
- Vistica, D. T.; Kenney, S.; Hursey, M. L.; Boyd, M. R. *Biochem. Biophys. Res. Commun.* **1994**, 200, 1762.
- Smith, A. M.; Dhawan, G. K.; Zhang, Z.; Siripurapu, K. B.; Crooks, P. A.; Dwoskin, L. P. *Biochem. Pharmacol.* **2009**, 78, 889.
- Rahman, S.; Neugebauer, N. M.; Zhang, Z.; Crooks, P. A.; Dwoskin, L. P.; Bardo, M. T. *Eur. J. Pharmacol.* **2008**, 601, 103.
- Albayati, Z. A.; Dwoskin, L. P.; Crooks, P. A. *Drug Metab. Dispos. Biol. Fate Chem.* **2008**, 36, 2024.
- Dwoskin, L. P.; Wooters, T. E.; Sumithran, S. P.; Siripurapu, K. B.; Joyce, B. M.; Lockman, P. R.; Manda, V. K.; Ayers, J. T.; Zhang, Z.; Deaciuc, A. G.; McIntosh, J. M.; Crooks, P. A.; Bardo, M. T. *J. Pharmacol. Exp. Ther.* **2008**, 326, 563.
- Rahman, S.; Zhang, Z.; Papke, R. L.; Crooks, P. A.; Dwoskin, L. P.; Bardo, M. T. *Br. J. Pharmacol.* **2008**, 153, 792.
- Zheng, G.; Zhang, Z.; Pivavarchyk, M.; Deaciuc, A. G.; Dwoskin, L. P.; Crooks, P. A. *Bioorg. Med. Chem. Lett.* **2007**, 17, 6734.
- Rahman, S.; Neugebauer, N. M.; Zhang, Z.; Crooks, P. A.; Dwoskin, L. P.; Bardo, M. T. *Neuropharmacology* **2007**, 52, 755.
- Lockman, P. R.; Manda, V. K.; Geldenhuys, W. J.; Mittapalli, R. K.; Thomas, F.; Albayati, Z. F.; Crooks, P. A.; Dwoskin, L. P.; Allen, D. D. *J. Pharmacol. Exp. Ther.* **2008**, 324, 244.
- Okuda, T.; Haga, T. *Neurochem. Res.* **2003**, 28, 483.
- Okuda, T.; Haga, T.; Kanai, Y.; Endou, H.; Ishihara, T.; Katsura, I. *Nat. Neurosci.* **2000**, 3, 120.
- Chang, C.; Ray, A.; Swaan, P. *Drug Discovery Today* **2005**, 10, 663.
- Cramer, R. D.; Patterson, D. E.; Bunce, J. D. *J. Am. Chem. Soc.* **1988**, 110, 5959.
- Geldenhuys, W. J.; Lockman, P. R.; McAfee, J. H.; Fitzpatrick, K. T.; Van der Schyf, C. J.; Allen, D. D. *Bioorg. Med. Chem. Lett.* **2004**, 14, 3085.
- Geldenhuys, W. J.; Lockman, P. R.; Nguyen, T. H.; Van der Schyf, C. J.; Crooks, P. A.; Dwoskin, L. P.; Allen, D. D. *Bioorg. Med. Chem.* **2005**, 13, 4253.
- Takasato, Y.; Rapoport, S. I.; Smith, Q. R. *Am. J. Physiol.* **1984**, 247, H484.
- Smith, Q. R. *Pharm. Biotechnol.* **1996**, 8, 285.
- Smith, Q. R.; Nagura, H.; Takada, Y.; Duncan, M. W. *J. Neurochem.* **1992**, 58, 1330.
- Lockman, P. R.; Roder, K. E.; Allen, D. D. *J. Neurochem.* **2001**, 79, 588.
- Lockman, P. R.; McAfee, J. H.; Geldenhuys, W. J.; Allen, D. D. *Neurochem. Res.* **2004**, 29, 2245.
- Lockman, P. R.; Gaasch, J.; McAfee, G.; Abbruscato, T. J.; Van der Schyf, C. J.; Allen, D. D. *Neurochem. Res.* **2006**.
- Momma, S.; Aoyagi, M.; Rapoport, S. I.; Smith, Q. R. *J. Neurochem.* **1987**, 48, 1291.
- Smith, Q. R.; Momma, S.; Aoyagi, M.; Rapoport, S. I. *J. Neurochem.* **1987**, 49, 1651.
- Allen, D. D.; Lockman, P. R. *Life Sci.* **2003**, 73, 1609.
- Lerner, J. *Comp. Biochem. Physiol.* **1989**, 93, 1.
- Simon, J. R.; Mittag, T. W.; Kuhar, J. M. *Biochem. Pharmacol.* **1975**, 24, 1139.
- Guyenet, P.; Lefresne, P.; Rossier, J.; Beaujouan, J. C.; Glowinski, J. *Mol. Pharmacol.* **1973**, 9, 630.
- Holden, J. T.; Rossier, J.; Beaujouan, J. C.; Guyenet, P.; Glowinski, J. *Mol. Pharmacol.* **1975**, 11, 19.
- Martin, K. *Br. J. Pharmacol.* **1969**, 36, 458.
- Simon, J. R.; Kuhar, M. G. *Nature* **1975**, 255, 162.
- Binda, C.; Newton-Vinson, P.; Hubalek, F.; Edmondson, D. E.; Mattevi, A. *Nat. Struct. Biol.* **2002**, 9, 22.
- Dowdall, M. J.; Barrantes, F. J.; Stender, W.; Jovin, T. M. *J. Neurochem.* **1976**, 27, 1253.
- Allen, D. D.; Geldenhuys, W. J. *Life Sci.* **2006**, 78, 1029.
- Cho, S. J.; Tropsha, A. *J. Med. Chem.* **1995**, 38, 1060.